VIROLOGICA SINICA, August 2009, 24 (4):333-349
DOI 10.1007/s12250-009-3055-y

CLC number: R373 Document code: A Article ID: 1674-0769 (2009) 04-0333-17

Involvement of Lipid Rafts and Cellular Actin in AcMNPV GP64 Distribution and Virus Budding*

F. J. Haines[1#], C. M. Griffiths[1], R. D. Possee[2], C. R. Hawes[1] and L. A. King [1**].

(1. School of Life Science, Oxford Brookes University, Oxford, OX3 0BP, UK; 2. NERC Centre for Ecology & Hydrology (Oxford), Mansfield Road, Oxford, OX1 3SR, UK.)

Abstract: GP64 is the major envelope glycoprotein associated with the budded virus (BV) of *Autographa californica* nucleopolyhedrovirus (AcMNPV) and is essential for attachment and budding of BV particles. Confocal microscopy and flotation assays established the presence of lipid raft domains within the plasma membranes of AcMNPV-infected Sf9 cells and suggested the association of GP64 with lipid rafts during infection. GP64 and filamentous actin (F-actin) were found to co-localise at the cell cortex at 24 and 48 hpi and an additional restructuring of F-actin during infection was visualised, resulting in a strongly polarised distribution of both F-actin and GP64 at the cell cortex. Depletion of F-actin, achieved by treatment of Sf9 cells with latrunculin B (LB), resulted in the redistribution of GP64 with significant cytoplasmic aggregation and reduced presence at the plasma membrane. Treatment with LB also resulted in reduced production of BV in Sf9 cells. Analysis of virus gene transcription confirmed this reduction was not due to decreased trafficking of nucleocapsids to the nucleus or to decreased production of infectious progeny nucleocapsids. Reduced BV production due to a lack of GP64 at the plasma membrane of AcMNPV-infected Sf9 cells treated with LB, suggests a key role for F-actin in the egress of BV.

Key words: *Autographa californica* nucleopolyhedrovirus (AcMNPV); Actin; Lipid rafts; Egress

During infection of insect cells with the baculovirus *Autographa californica* nucleopolyhedrovirus (AcMNPV), budded virus (BV) attaches to susceptible insect cells via interactions of the major surface glycoprotein GP64 with host cellular receptors (25), following which the BV particle enters the cell via adsorptive endocytosis (72). GP64 facilitates fusion of the viral envelope with the endosomal membrane (7, 49, 50), releasing the nucleocapsid into the cytoplasm. Trafficking of nucleocapsids to the nucleus is thought to be mediated by the formation of actin cables (F-actin), and major re-distribution of this cytoskeletal filament has been shown to occur during the early stages of infection (13, 14, 17, 34, 43, 44, 53, 70). Progeny nucleocapsids produced within the nucleus

Received: 2009-01-31, Accepted: 2009-05-18

* Foundation items: This work was partially supported by a BBSRC grant (LAK, RDP) and by a BBSRC-funded PhD studentship (FJH).

Current address: Veterinary Laboratories Agency-Weybridge, New Haw, Addlestone, Surrey, KT15 3NB, UK.

** Corresponding author.
Phone: +44-1865-483241, Fax: +44-1865-483242,
E-mail: laking@brookes.ac.uk

are trafficked to the plasma membrane via an unknown mechanism, to distinct areas of the membrane rich in GP64 (46, 72). Here, nucleocapsids bud through the plasma membrane, acquiring a host-derived envelope enriched in GP64 at one end (6, 72).

GP64 undergoes post-translational modifications including N-glycosylation (12, 28, 47, 72, 73) and palmitoylation (52, 75). Release of BV is concomitant with the localisation of GP64 in distinct loci at the plasma membrane (6) and deletion of *gp64* results in a 98% reduction in BV production (46). Surface glycoproteins of other enveloped viruses such as HIV (29, 31, 38, 45), measles (39, 69) and influenza (36, 57, 66), are anchored within structured patches of the plasma membrane. These domains are enriched in cholesterol and sphingolipids and are commonly referred to as lipid rafts or, in the context of virus exit from cells, as budding domains (20, 59). Biochemical analysis of the proteins associated with lipid rafts show that post-translational modifications such as palmitoylation (15, 41, 51, 58) may be important for targeting to rafts and in some cases appears to be essential for raft localisation (5, 37, 54). Zhang *et al*. (75) has demonstrated palmitoylation of AcMNPV GP64, but showed that prevention of GP64 palmitoylation did not substantially affect synthesis or transport of GP64 to the plasma membrane.

During AcMNPV infection of Sf9 cells, we have shown GP64 co-localisation with areas of the infected cell plasma membrane enriched with the ganglioside GM_1. Furthermore, we have demonstrated GP64 incorporation into detergent-resistant, buoyant membrane fractions derived from infected Sf9 cells at times up to 48 hpi. The demonstration that F-actin also appeared to co-localise with GP64 at the plasma membrane led us to examine the role of F-actin during virus egress. A number of viruses are known to manipulate host F-actin during virus budding, including vaccinia virus (reviewed in 62) and HIV (22). Furthermore, the haemagglutinin (HA) surface glycoprotein of influenza relies on the host actin cytoskeleton to maintain correct organisation of lipid rafts for incorporation of HA into budding virus particles (61). Although the re-organisation and involvement of F-actin during the early stages of AcMNPV infection of insect cells has been studied in detail (13, 17, 34, 43, 44, 53, 70), relatively little is known about the involvement, if any, of the actin cytoskeleton during virus egress and budding. We have demonstrated a re-organisation of F-actin to co-localise with GP64 at the plasma membrane during the late stages of AcMNPV infection. Depletion of F-actin using the drug Latrunculin B (LB) reduced BV production and prevented incorporation of GP64 within discrete domains of the plasma membrane. Examination of virus gene expression and the infectivity of occlusion bodies confirmed that the reduction of BV yield was not a consequence of reduced trafficking of nucleocapsids to the nucleus following infection nor of interference with the production of infectious nucleocapsids.

METHODS

Cell lines and viruses

Spodoptera frugiperda Sf9 cells were cultured at 28℃ in Sf900II medium (Invitrogen, UK). *Autographa californica* nucleopolyhedrovirus (AcMNPV) clone 6 was used in this study (2).

Detergent extraction and membrane flotation assays

Five-fraction flotation gradients were performed

following a modification of the protocol of Lindwasser and Resh (38). Sf9 cells were infected with AcMNPV at a multiplicity of infection (MOI) of 20 PFU/cell and at 24, 48 and 72 hpi, 3×10^6 cells were harvested in a bench-top centrifuge (1 000×g, 10 min, 4℃) and resuspended in 42μL TNET buffer (50mmol/ L Tris-HCl, pH 7.4; 150mmol/L NaCl; 5mmol/L EDTA; 0.5%Triton X-100). Cholesterol-enriched membranes were extracted by incubation on ice for 30 minutes in this buffer, and samples were adjusted to 30% v/v Optiprep™ (Axis Shield, UK) in TNET buffer. One third of the cell extract (84μL) was placed in a micro ultra-centrifuge tube and overlaid with 1.2mL of 30% Optiprep™ and 70μL TNET buffer. Following centrifugation at 170 000×g at 4℃ for 4 h, five 280μL samples were collected in series from the top to the bottom of the gradient. The proteins in each fraction were precipitated with 20% trichloroacteic acid and separated on a 12% SDS-PAGE gel. Following transfer onto nitrocellulose membrane, fractions were probed with monoclonal anti-GP64 (1:200 dilution; a gift from Loy Volkman, University of Berkley, California, USA) or anti-caveolin-1 (dilution 1:50; Santa Cruz Biotechnology, UK) antibody, and antibody binding was detected with alkaline phosphatase conjugated secondary antibody (Sigma Aldrich, UK).

Immunostaining of insect cells

Sf9 cells were seeded onto 13mm glass coverslips in 35mm tissue culture dishes (cell density 1×10^6 cells/dish) and infected with AcMNPV at MOI of 10 PFU/cell. Control cells were left uninfected. At various times post infection cells were fixed with 4% paraformaldehyde in PEM buffer (0.1mol/L PIPES, pH 6.9, 10mmol/L EGTA, 10mmol/L $MgCl_2$) and treated with permeabilisation buffer (0.1mol/L PIPES, pH 6.9, 0.1% Triton X-100, 2% BSA) prior to antibody staining. Actin structures were fixed prior to antibody staining by incubating cells for 15 min in MBS buffer (0.1mol/L PIPES, pH 6.9, 10mmol/L EGTA, 10mmol/L $MgCl_2$, 100mmol/L maleimidobenzoic acid N-hydroxysucinimide ester, 0.1% Triton X-100), to stabilise actin structures (48). Samples were incubated for 20 min with media containing 2μg/mL cholera toxin subunit B Alexa Fluor 594 conjugate or 1 Ut/mL Alexa Fluor 594 phalloidin (Molecular Probes, UK). Immunostaining of GP64 was carried out as previously described (68) using monoclonal GP64 antibody as above. Coverslips were washed with PBS and mounted onto slides using Citifluor (Agar Scientific, UK). All samples were imaged using a Zeiss LSM 510 Laser Scanning Confocal Microscope.

Analysis of virus production in the presence of Latrunculin B

Replicate Sf9 shake cultures (30mL) were established at 1.5×10^6 cells/mL and incubated for 24 h in the presence or absence of 0.4μg/mL LB. All cultures were analysed and cell densities adjusted to 2×10^6 cells/mL with medium containing or lacking LB, as appropriate. Cultures were infected with AcMNPV at MOI of 20 PFU/cell and at 1 hpi infected cultures were washed with appropriate medium (with or without LB) to remove unbound virus. Washed cell pellets were resuspended in fresh medium either with or without 0.4μg/mL LB. Cultures that had not been treated with LB prior to infection, and that remained free of drug during virus replication were designated LB-- and served as controls. Cultures treated with LB prior to infection and also treated with LB from 1 hpi

were designated LB++. Cultures treated with LB prior to infection, but washed free of drug following infection were designated LB+-. Cultures not treated with LB prior to infection, but which received LB at 7 hpi were designated LB-+. Infected culture medium was harvested from each culture at various times post infection and stored at 4℃. Cells were also harvested at these times, pelleted and stored at -20℃.

Reverse Transcriptase Polymerase Chain Reaction

Total cell RNA from 2×10^6 AcMNPV-infected Sf9 cells from the above experiment was extracted using QIAGEN RNeasy® Mini Kits. Reverse transcription of extracted RNA samples used an oligo $dT_{(14)}$ primer (Invitrogen, UK) and the Omniscript® RT kit (Qiagen, UK) according to manufacturer's protocols. Virus gene-specific cDNAs were amplified by PCR using 2μL of the RT reaction and standard oligonucleotide primers for three viral genes, immediate early 2 (*ie2*), viral capsid protein 39 (*vp39*) and DNA polymerase (*dnapol*). PCR products were visualised by agarose gel electrophoresis.

Occlusion body extraction and infection of insect larvae

Occlusion bodies (OBs) from cell pellets of Sf9 cells infected with AcMNPV in the presence or absence of LB were harvested (32). Third instar *Trichoplusia ni* larvae were inoculated with a range of doses of OBs using the diet-plug method (32) and monitored daily for pupation or virus death. Data were analysed using GraphPad Prism 4 software, version 4.03.

RESULTS

Analysis of GP64 and cellular membrane domains

The glycoproteins of a number of enveloped viruses associate with lipid rafts during infection (29, 31, 36, 38, 45, 57, 66). These detergent-resistant membrane domains have been shown in a variety of insect cells (1, 25, 65, 74, 75). Flotation gradients were used to analyse lipid raft-associated proteins in AcMNPV-infected Sf9 cells. Western blot analysis confirmed the presence of caveolin-1, a protein known to localise within cholesterol-enriched raft domains in Sf9 cells (1), in both non-infected and AcMNPV-infected insect cells (data not shown). Flotation gradients of AcMNPV-infected insect cells harvested at 24 hpi (Fig. 1A) demonstrated localisation of caveolin-1 within fractions 1 and 5 of the flotation gradient, corresponding to the lipid raft fraction and soluble fraction respectively, a distribution typical of raft-associated proteins (9). Typically, proteins that become enriched within lipid rafts are detected in the upper-most fraction (fraction 1) of flotation gradients, due to the buoyant density of cholesterol-enriched rafts and their associated proteins. Conversely, membrane proteins not associated with raft domains are solubilised during detergent extraction and remain in the lower fractions. Analysis of the protein content of each fraction at 24 hpi (Fig. 1B) detected GP64 in all fractions of the gradient including fraction 1. By 48 hpi (Fig. 1C), the majority of GP64 was detected in fraction 1 and at 72 hpi (Fig. 1D) GP64 was only detected in fraction 1. The detection of GP64 in fraction 1 at all times post-infection suggests the incorporation of GP64 into detergent-resistant, cholesterol-enriched domains of the plasma membrane of AcMNPV-infected Sf9 cells. Detection of GP64 in other fractions of the flotation gradient at 24 and 48 hpi is likely to reflect the high levels of nonmembrane associated GP64 within AcMNPV-infected Sf9 cells at these times, as continuous synthesis and trafficking distributes high levels of this protein throughout

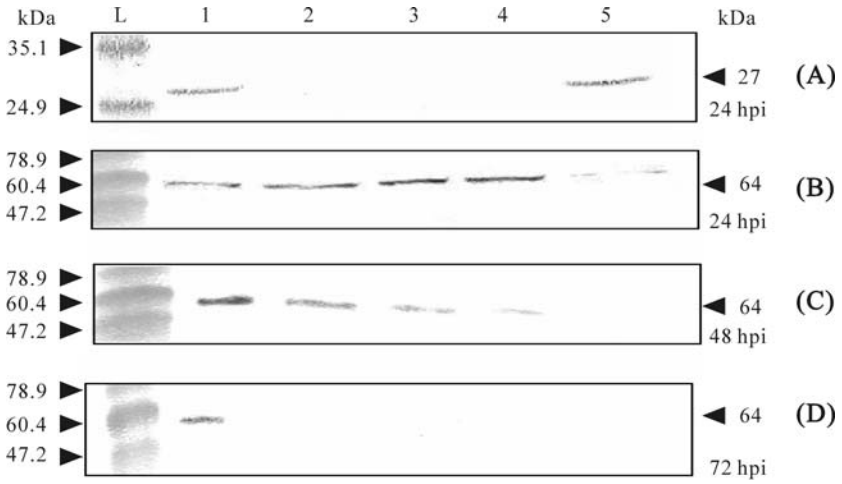

Fig. 1. Detection of AcMNPV GP64 in lipid raft-containing membrane fractions of Sf9 cells by flotation gradients. AcMNPV-infected Sf9 cells were harvested at 24 (A, B), 48 (C) or 72 (D) hpi and following lysis, cholesterol-rich membrane regions were separated by flotation analysis (fraction 1) from other cellular components (fractions 2-5). Fractions 1 – 5, obtained from flotation gradients for each cell sample, were analysed for protein content by Western blot detection with antibody specific for the lipid raft-associated protein caveolin-1 (A) or for AcMNPV GP64 (B to D). Protein molecular weight markers are indicated in kDa (L).

the ER and Golgi during infection. At 72 hpi GP64 synthesis has all but ceased, and the remaining cell-associated GP64 has likely been transported to the plasma membrane. The presence of GP64 solely in fraction 1 of the flotation gradient at this time (Fig. 1D) suggests GP64 continues to be associated with lipid rafts.

To confirm the localisation of GP64 within raft domains of AcMNPV-infected Sf9 cells, dual immunostaining and confocal microscopy were used to visualise the distribution of lipid rafts and GP64 throughout infection (Fig. 2). Cholera toxin subunit B (CTxB) binds to galactosyl moieties such as the ganglioside GM_1, a well-characterised marker of raft domains (3, 33, 40), thereby indicating the distribution of raft domains across the membrane. Staining of non-infected Sf9 cells with Alexa Fluor 594-conjugated CTxB (Molecular Probes) revealed GM_1-rich domains distributed across the plasma membrane in a random, punctate distribution (Fig. 2A), consistent with findings from mammalian cells (10). Dual immunostaining of AcMNPV-infected Sf9 cells at 24 hpi demonstrated both CTxB (raft domains) and GP64 distributed evenly across the membrane in both surface-view (data not shown) and in cross-section (Fig. 2B). GP64 stained as a random, punctate distribution reminiscent of the CTxB staining pattern observed in uninfected cells. The CTxB staining in infected cells at 24 hpi appeared more intense than for uninfected cells and tended to obscure the punctate pattern, making true localisation difficult to discern. By 48 hpi (Fig. 2C), the levels of both CTxB and GP64 had fallen in infected cells, and both revealed a concentrated re-distribution at one edge of the cell where co-localisation of the two proteins was readily visible. CTxB was detectable in punctuate distribution at other parts of the plasma membrane but little GP64 was visible except at the region of co-localisation. By 72 hpi (Fig. 2D), staining for both proteins was weak, with the distribution of GM_1-rich domains retaining a

punctate distribution, and minimal GP64 associated with the cell periphery. These results concur with Fig. 1, suggesting the association of GP64 with cholesterol-enriched, detergent-resistant regions of the plasma membrane enriched in GM_1.

Co-localisation of F-actin and GP64 in insect cells during very late infection

The actin cytoskeleton is known to interact directly with raft-associated proteins (11, 55, 61, 64) and thickens at the insect cell cortex during AcMNPV-infection. The distribution of F-actin and GP64 during late stages of AcMNPV infection were visualised with Alexa Fluor 594-conjugated phalloidin (Molecular Probes) and anti-GP64 antibody, respectively (Fig. 3). F-actin distribution in uninfected Sf9 cells (Fig. 3A) showed actin cables within microspikes projecting from the cell surface in an even distribution across the cell surface when viewed from a ventral plane (Fig. 3A). When viewed in a medial plane, uninfected cells displayed a faint ring of F-actin under the plasma membrane of variable intensity (Fig. 3B), with some degree of irregular cytoplasmic staining. No GP64 staining

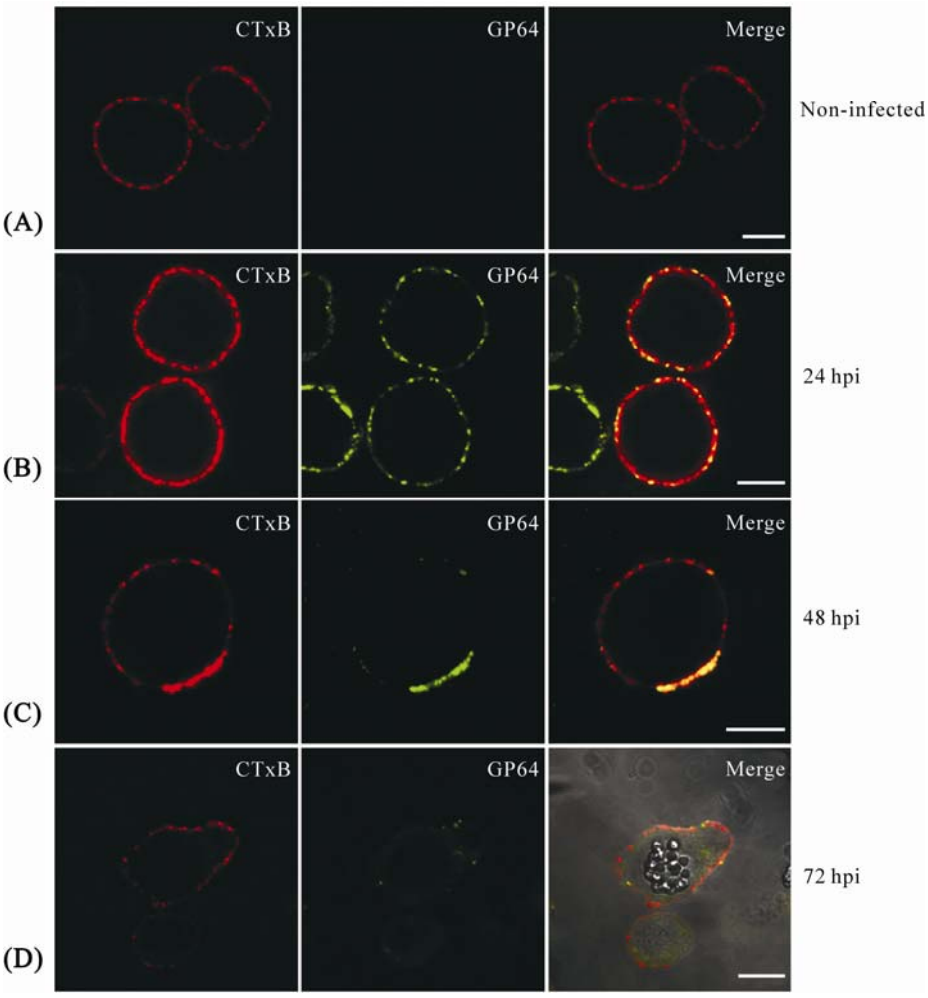

Fig. 2. Co-localisation of GP64 and GM_1-rich domains in uninfected and AcMNPV-infected Sf9 cells by dual immunostaining and confocal microscopy. Uninfected (A) and AcMNPV-infected Sf9 cells at 24 (B), 48 (C) and 72 (D) hpi were labelled with cholera toxin subunit B Alexa Fluor 594 conjugate (CTxB; red; left panel), monoclonal anti-GP64 IgG and rabbit anti-IgG FITC conjugate (GP64; green, middle panel). Merging of the two images (merge, right panel) reveals co-localisation of anti-GP64 antibody and CTxB staining (yellow). (Scale bar = 10μm)

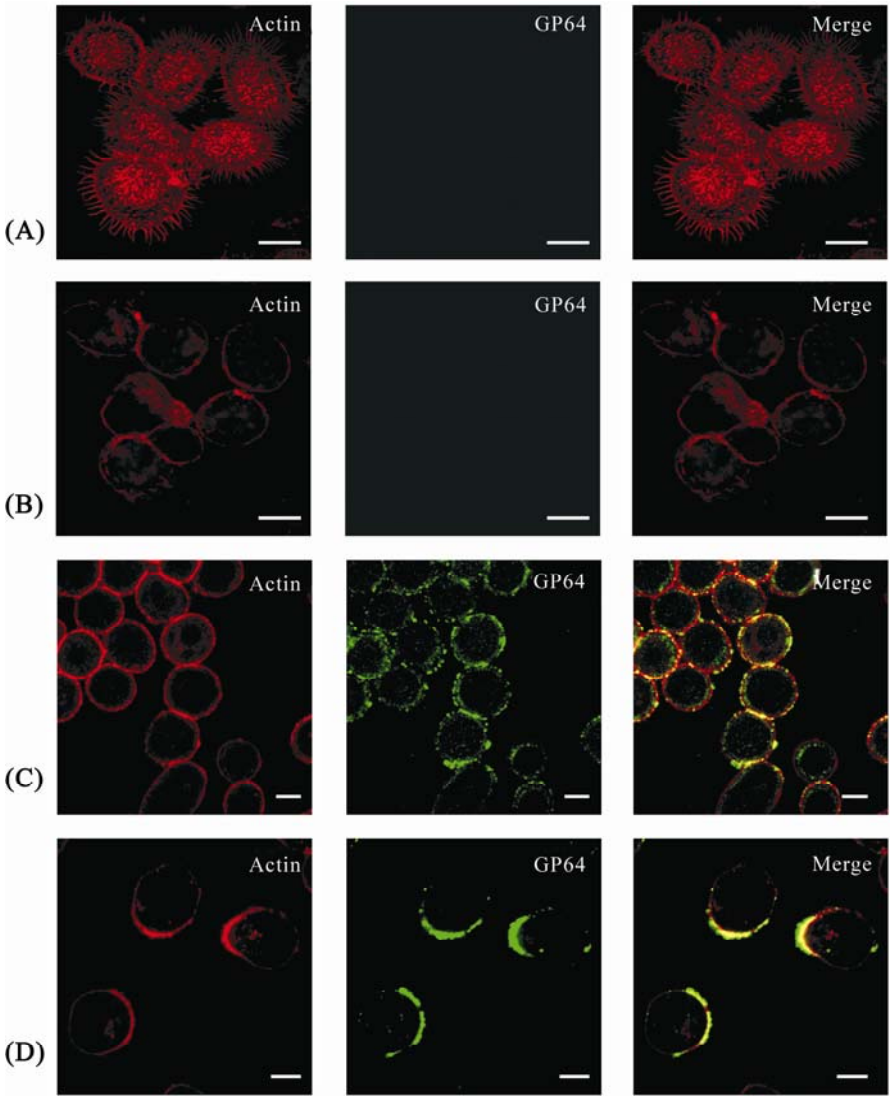

Fig. 3. Co-localisation of F-actin and GP64 distribution in uninfected and AcMNPV-infected Sf9 cells by dual immunostaining and confocal microscopy. Uninfected Sf9 cells (A, B) and AcMNPV-infected cells at 24 (C), 48 (D) hpi were labelled with Alexa Fluor 594-conjugated phalloidin (Actin; red; left panel), monoclonal anti-GP64 IgG and rabbit anti-IgG FITC conjugate (GP64; green, middle panel). Merging of the two images (merge, right panel) reveals co-localisation of anti-GP64 antibody and phalloidin staining (yellow). Uninfected Sf9 cells are viewed in both the ventral (A) and medial (B) planes. Infected cells (C, D) are viewed medially. (Scale bar = 10μm)

was visible in uninfected cells. At 24 hpi (Fig. 3C), F-actin demonstrated a more universal distribution, with thickened staining under the cell cortex compared to uninfected samples (see Fig. 3B). GP64 at 24 hpi demonstrated a predominantly punctuate distribution across the plasma membrane, as in Figure 2B, and at several locations GP64 appeared to co-localise with F-actin under the lipid bilayer, although the thickened actin layer made co-localisation difficult to confirm. By 48 hpi (Fig. 3D) both F-actin and GP64 illustrated a polarisation toward one edge of the cell and GP64 appeared to completely co-localise with F-actin at this time. This phenomenon was also observed when staining for GP64 alone (data not shown). The results strongly reflect the data for lipid raft and GP64 re-distribution at 48 hpi (Fig. 2C), indicating an association

between GP64, actin and lipid rafts during infection, and supporting the observation that budding occurs from discrete areas of the plasma membrane enriched in GP64 (46, 72). The exact nature of the association between GP64 and F-actin is unknown but the co-localisation of GP64 and F-actin, and of GP64 and lipid rafts at the cell cortex suggest a possible role for both lipid rafts and F-actin during budded virus egress.

Depletion of cellular F-actin following treatment of Sf9 cells with Latrunculin B

Latrunculin B (LB) has been used to study the role of actin in the assembly, egress and release of a number of viruses (4, 16, 18, 23). LB rapidly and reversibly binds to G-actin monomer in cells *in vitro* (63), ultimately resulting in the net depolymerisation of the F-actin network within treated cells. Previous research into the role of F-actin in AcMNPV trafficking and morphogenesis has employed cytochalasin D (CD), an alternative actin-depolymerising drug. Treatment of Sf21 and *Trichoplusi ni* (*T ni*) 368 cells with CD does not result in the net depolymerisation of F-actin seen with Latrunculin A (LA) (30), but rather culminates in the formation of cytoplasmic aggregates (30, 67). To ensure complete depolymerisation of F-actin within insect cells, non-infected Sf9 cells were treated with LB for 24 hours and stained with Alexa Fluor 594-conjugated phalloidin (Fig. 4A). Following LB treatment, minimal F-actin could be visualised within the cell cytoplasm or at the cell membrane compared to untreated cells (Fig. 4B), and no microspikes could be seen on the surface (data not shown). These results were comparable to insect cells treated with LA for 25 h (30) and illustrated the complete abrogation of cellular F-actin by LB in Sf9 cells.

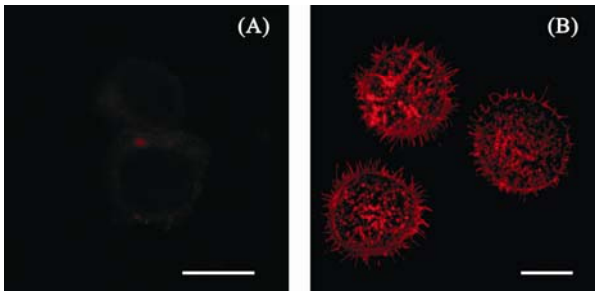

Fig. 4. Depletion of F-actin by Latrunculin B treatment of Sf9 cells. Uninfected Sf9 cells were treated for 24 h with 0.4μg/mL Latrunculin B (LB) (A) and stained with Alexa Fluor 594-conjugated phalloidin (Molecular Probes, UK). Absence of staining, compared to untreated Sf9 cells (B), demonstrated LB treatment resulted in a total loss of F-actin from cells. (Scale bar = 10μm).

Distribution of GP64 in insect cells during Ac-MNPV infection in the presence of LB

The effect of F-actin depolymerisation on GP64

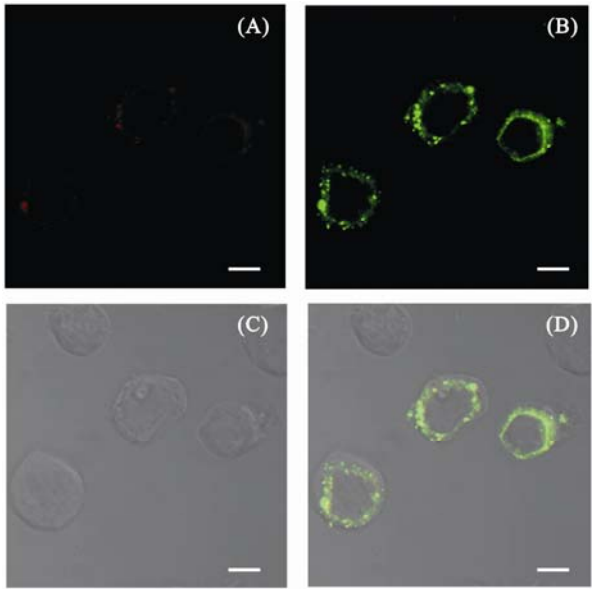

Fig. 5. Redistribution of GP64 in AcMNPV-infected Sf9 cells following F-actin depletion by treatment with Latrunculin B at 7 hpi. Sf9 cells were infected with AcMNPV at an MOI of 10 PFU/cell and treated with 0.4μg/mL Latrunculin B at 7 hpi. Cells at 24 hpi were fixed and stained with Alexa Fluor 594-conjugated phalloidin (red; panel A), monoclonal anti-GP64 IgG and rabbit anti-IgG FITC conjugate (green; panel B). Panel C illustrates the same view using transmitted light. Panel D represents a merged image of panels A, B and C. (Scale bar = 10μm).

distribution during infection is shown in Figure 5. Roncarati and Knebel-Mörsdorf (53) demonstrated that F-actin cables, extending from the plasma membrane into the cytoplasm of insect cells as a consequence of baculovirus nucleocapsid entry, were no longer visible by 6 hpi suggesting that the trafficking of nucleocapsids to the nucleus had ceased by this time. We therefore predicted that the addition of LB at 7 hpi would be unlikely to adversely affect virus entry or trafficking of nucleocapsids to the nucleus. Sf9 cells were infected with AcMNPV and treated with LB from 7 hpi. Cells were fixed at 24 hpi and stained with anti-GP64 antibody and Alexa Fluor 594-conjugated phalloidin. Cells treated with LB from 7 hpi demonstrated an extremely low, randomlydistributed staining for F-actin (Fig. 5A). In comparison with untreated cells stained with Alexa Fluor 594 phalloidin (see Fig. 3), the low levels of fluorescence in these cells shows no filamentous network within the cytoplasm or under the cell cortex, indicating an almost complete absence of F-actin at 24 hpi. The fluorescence detected in Figure 5A may indicate some aggregation of actin within the cytoplasm, a phenomenon often described following the addition of the drug CD (67). GP64 appeared to accumulate within the cytoplasm of LB-treated cells (Fig. 5B), whereas in infected cells that had not been treated with LB (Fig. 2C, 3C) the distribution of GP64 was predominantly at the plasma membrane, as expected from Figure 3. Transmitted light microscopy confirmed the viability of the cell was maintained during drug treatment (Fig. 5C). The merged image indicated that co-localisation of F-actin and GP64 staining was absent (Fig. 5D). Treatment of Sf9 cells with LB disrupted the cellular F-actin network and resulted in a re-distribution of GP64, suggesting a role for actin in the targeting of GP64 to the plasma membrane.

Effect of Latrunculin B on budded virus production

Little is known about the trafficking of nucleocapsids during baculovirus egress but a potential role is suggested for F-actin from our results above, which lead us to examine BV production in the presence (+) or absence (-) of LB. Sf9 cells were infected with AcMNPV and treated with LB at different times during the experiment. Yields of extracellular BV were determined by titration of culture media from infected cells at 24 hpi as previously described (32) (Fig. 6).

Production of BV by infected cells that remained untreated throughout the experiment (LB--; Fig. 6A) reached an average titre of 1.18×10^7 PFU/mL at 24 hpi. Cells that had been treated with LB only from 7 hpi (LB-+; Fig. 6B) demonstrated significantly reduced BV yields, approximately 100-fold lower than untreated (LB--) control cells, with a mean titre of 1.2×10^5 PFU/ mL. In cells treated with LB continuously for the 24 h prior to infection and throughout the 24 h infection period, (LB++; Fig. 6C), BV production was also severely compromised, with a low mean titre of 5.7×10^4 PFU/mL, similar to that of cells treated with LB from 7 hpi (LB-+; Fig. 6B). Finally, cells that were treated with LB for 24 hours prior to infection, but were washed to remove the drug after incubation with virus and subsequently incubated free of LB for the remainder of the experiment (LB+-; Fig. 6D), produced a mean titre of 1.2×10^7 PFU/mL at 24 hpi, which was comparable to the untreated control samples LB--. ANOVA analysis of raw data showed a significant difference between all samples (Fig.6 A to D) ($P<0.0001$). T-test analysis for BV titres from LB-- (untreated) and LB+- (treated only prior to infection)

samples demonstrated no significant difference between BV yields (Fig. 6A and 6D; P = 0.899), which remained high. Likewise, t-test analysis for BV titres from LB++ (treated both prior to and after infection) and LB-+ (treated only from 7 hpi) cells also demonstrated no significant difference between BV titres (Figure 6B and 6C; P = 0.213) although both gave severely reduced titres compared to the control. Treatment of cells with LB prior to infection followed by subsequent incubation in drug-free conditions (LB+-) demonstrated no reduction of BV egress, suggesting that the elimination of cellular F-actin prior to, and during the infection stage, was not detrimental to virus entry into these cells. Conversely, cells treated with LB throughout the course of the virus infection demonstrated drastic reductions in the titre of BV detected.

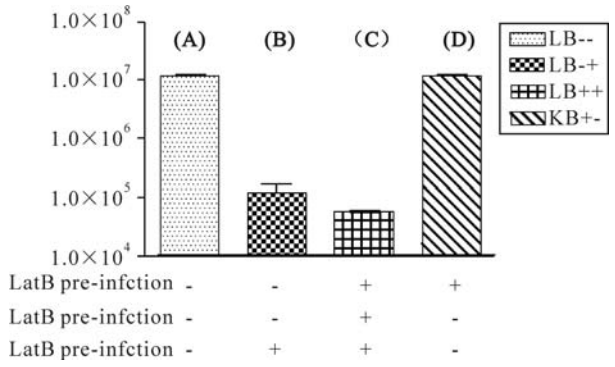

Fig. 6. Budded virus titres at 24 hpi in the presence or absence of Latrunculin B. Sf9 cultures at 1.5×10^6 cells/mL were incubated with or without 0.4μg/mL LB for 24 h and cell densities adjusted to 2×10^6 cells/mL prior to infection with AcMNPV at MOI of 20 PFU/cell. Infected culture media were harvested at 24 hpi and BV titres determined by plaque assay. Control cultures remained free of drug during the whole experiment (LB--; A). Three drug treatment regimes were used. Cells were either (i) treated with LB only from 7 hpi (LB-+; B), (ii) were treated with drug throughout the whole experiment (LB++; C) or (iii) were treated with LB for 24 h prior to virus infection, but then incubated in medium free of drug from 1 hpi (LB+-; D). Titres are indicated in PFU/mL and are the mean of three replicates for each treatment.

The inhibition of BV production by LB-induced F-actin depletion occurred when the drug was present at all times during the experiment (LB++), but critically also occurred when the drug was only applied at several hours post-infection (LB-+; Fig. 6C). The results suggest that the absence of F-actin during late, but not early, stages of AcMNPV infection of Sf9 cells affected the production of BV at 24 hpi to the greatest degree. Reduced BV production was affected by the loss of F-actin from 7 hpi irrespective of prior drug treatment or otherwise and was associated most closely with the abrogation of F-actin formation by LB treatment of cells post infection (LB-+ and LB++; Fig. 6B and 6C), rather than with LB treatment prior to infection (LB+-; Fig. 6D). These data implied that reduced BV production at 24 hpi was a consequence of events following virus replication within the nucleus, rather than an inhibition of virus entry at the very stages times in infection. To attempt to verify this, virus gene expression was examined in these cells.

Effect of Latrunculin B treatment of transcription of viral genes

To determine if the reduction in BV production was a consequence of restricted trafficking of nucleocapsids to the nucleus following initial infection stages, reverse transcriptase PCR (RT-PCR) was employed to analyse transcription of selected viral genes. The genes identified for analysis were the immediate early 2 (*ie2*), DNA polymerase (*dnapol*) and viral capsid protein 39 (*vp39*) genes and transcription profiles of all cells treated with LB were compared to untreated LB-- cells by agarose gel electrophoresis.

RT-PCR analysis of *ie2* gene transcription for untreated cells (LB--; Fig.7A) demonstrated transcription from 1 hpi to 24 hpi with an apparent peak of

transcription at 4 hpi. All LB-treated samples demonstrated similar levels of *ie2* transcription from 1 to 24 hpi compared to LB--, although transcription levels of *ie2* appeared to be marginally greater at 4 hpi for LB+- and marginally reduced at 1 hpi for LB++. Analysis of *dnapol* and *vp39* for untreated cells demonstrated transcription from 4 hpi and 8 hpi, respectively (Fig. 7B and 7C) and revealed comparable timings and levels of transcription for these genes in all four samples. These results indicate that treatment with LB (and therefore depletion of F-actin) had no gross effects on selected virus gene transcription from 1 to 24 hpi. Cells treated either prior to infection (LB+-), after infection (LB-+), or throughout the experiment (LB++) demonstrated almost identical expression profiles for *ie2*, *dnapol* and *vp39* genes compared to untreated control cells. These results confirmed that the absence of cytoplasmic and nuclear F-actin does not inhibit or restrict trafficking of nucleocapsids to the nucleus during initial infection processes, and that the reduction of BV yield associated with F-actin depletion was not a consequence of reduced, inhibited or delayed virus replication within the cell.

Effect of Latrunculin B on occlusion body production and infectivity

Talhouk and Volkman (67) observed a delay in the synthesis of polyhedrin following addition of CD to AcMNPV-infected insect cells. To analyse the effects of LB on occlusion body (OB) production and infectivity, Sf9 cells were treated with LB as described above, and OBs harvested from cells at 48 hpi. The infectivity of OBs was determined using oral infection of third instar *T. ni* larvae. Statistical analyses of lethal dose (LD_{50} and LD_{95}) and survival time revealed no significant differences between the infectivity of OBs produced in Sf9 cells treated with LB at any time prior to or during infection with AcMNPV, compared to untreated AcMNPV-infected cells (Table 1). No significant reduction of OB infectivity *in vivo* as determined by these parameters was found when Sf9 cells were treated with LB using

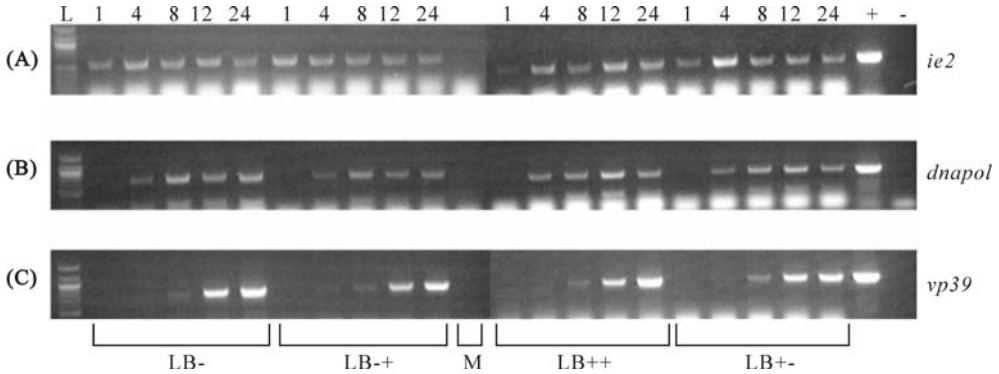

Fig. 7. Selected virus gene expression in AcMNPV-infected cells in the presence or absence of Latrunculin B. Total RNA was extracted at various times post infection from Sf9 cells infected with AcMNPV under one of the three LB treatment regimes described (LB-+, LB++, LB+-), or from AcMNPV-infected Sf9 cells that had not been treated with LB (LB--). Reverse transcriptase was carried out on all RNA samples, and cDNA copies of viral transcripts were amplified by PCR using oligonucleotide primers designed to have specificity for the AcMNPV genes immediate early 2 (*ie2,* panel A), DNA polymerase (*dnapol,* panel B) and capsid (*vp39,* panel C). Controls include mock (uninfected Sf9 cells (M), virus DNA positive control (+), water negative control (-). Molecular weight marker is 100bp Ladder (L) from New England Biolabs.

Table 1. Infectivity of occlusion bodies produced in the presence or absence of Latrunculin B.

Sample type	Lethal dose (OB/larva)			Survival Time	
	LD_{50}	LD_{95}	*P*	dpi (SD)	*P*
LB --	16.02	731.3		7.6 (0.565)	
LB -+	38.78	1197.6	< 0.05	7.7 (0.47)	0.659
LB ++	7.34	533.8	< 0.5	7.4 (0.565)	0.098
LB +-	14.93	677.5	< 0.1	7.3 (0.562)	0.035

Occlusion bodies were extracted at 48 hpi from Sf9 cells infected with AcMNPV under one of the three LB treatment regimes described (LB-+, LB++, LB+-), or from AcMNPV-infected Sf9 cells that had not been treated with LB (LB--). OBs were quantified and used to infect third instar *Trichoplusia ni* (T. ni) larvae at a range of doses by the diet plug oral infection method. Lethal dose (LD_{50} and LD_{95}) values were determined by linear regression and P values compared to control samples (LB--) were determined using chi-square analysis. Survival times in days post infection (dpi) were also compared to control samples, using student's t-test analysis (http://www.physics.csbsju.edu/stats/t-test.html) to determine P values and standard deviation (SD).

any of the three regimes described (LB-+, LB++ or LB+-). Additionally, analysis of the DNA content of OBs produced by these cells revealed no detectable differences in the levels of viral DNA within the different OB sample types (data not shown). The absence of any detrimental effects of LB treatment on OB production and infectivity is strong evidence that the production and occlusion of infectious nucleocapsids is not affected in Sf9 cells by the absence of F-actin. These results support the conclusion that reduction of BV production following F-actin depletion was not due to the loss of virus genome replication or nucleocapsid assembly, indicating F-actin depletion did not affect virus replication.

DISCUSSION

Production of baculovirus progeny within an infected insect cell requires that the virus hijack the host cell cytoskeleton for intracellular trafficking of virus particles to and from the nucleus. Much research has focused on determining the synthesis, processing and functions of the major surface glycoprotein of the budded virus (BV), GP64. This protein is essential in both attachment of BV particles to susceptible cells (7, 42, 71) and release of progeny BV from infected cells (46). The results of confocal microscopy and membrane fractionation assays in this study provide evidence for the targeting of GP64 within cholesterol-enriched, raft-like domains during AcMNPV infection. Dual immunostaining of AcMNPV-infected Sf9 cells demonstrated the polarisation of both GP64 and GM_1-rich proteins at the plasma membrane at 48 hpi. Previous observations have suggested nuclear swelling, the subsequent polarisation of the Golgi apparatus and vesicle trafficking during AcMNPV infection as the primary reasons for this polarisation of GP64 (21, 35). Partitioning of certain proteins into lipid raft domains is thought to occur within the *trans* Golgi network (TGN) (8, 24, 26, 60) and GP64 is known to be post-translationally modified within the Golgi apparatus (6, 19, 27, 47), providing support for a possible mechanism for GP64 to likewise be incorporated into cholesterol-enriched raft domains at the TGN membrane. Following this incorporation, the polarisation of Golgi observed during infection of insect cells could lead to the subsequent trafficking of proteins to one edge of the plasma membrane as was seen in these cells. The polarisation and co-localisation of both GP64 and other integral lipid raft-associated proteins such as GM_1 (detected by CTxB staining) at

the cell surface was observed in the present study and supports the hypothesis that GP64 is trafficked to lipid raft domains in the plasma membrane of baculovirus-infected insect cells. Baculovirus budding has been shown to occur from discrete areas of the plasma membrane enriched in GP64 (46, 72), suggesting a link between the distribution of lipid rafts and virus egress, through the recruitment and positioning of GP64.

Using a similar gradient-based flotation assay, Zhang *et al*. (75) failed to detect GP64 in fractions predicted to contain lipid rafts, but in this study samples were only harvested at 72 hpi, when limited levels of GP64 remain within the cell (21). The present study used cells harvested at various times post-infection (24, 48 and 72 hpi) and clearly detected GP64 within the upper-most fraction (where detergent-resistant domains would be predicted) of gradient for all samples (Fig.1). Flotation assay results were supported by confocal microscopy, demonstrating the co localisation of lipid raft proteins and GP64 in AcMNPV-infected cells most clearly at 48 hpi (Figure 2C). Both assays demonstrated reduced levels of GP64 at 72 hpi (Fig. 1D and Fig. 2D), concomitant with both falling levels of GP64 synthesis in infected cells at later times post-infection and the continuous depletion of GP64 from virus-infected cells as nucleocapsids bud through the lipid bilayer during egress, incorporating GP64 into their envelope. At 72 hpi very low levels of GP64 were found associated with only the top fraction of the gradient, indicating that the glycoprotein had been lost from the cell following incorporation into BV. We suggest that Zhang *et al*. (75) may have failed to observe GP64 in lipid rafts at 72 hpi because of the very low levels of GP64 in the plasma membrane of infected cells at this time. Zhang and colleagues were able to detect their positive control at 72 hpi, the Fasciclin 1 (Fas I) lipid-raft associated protein from *Drosophila melanogaster* (76) but in contrast to GP64, Fasciclin 1 remains anchored in the plasma membrane of the cell throughout infection, thereby remaining at higher levels in the membrane.

Confocal microscopy of cells at late times post-infection demonstrated a co-localisation of F-actin and GP64 in AcMNPV-infected Sf9 cells from 24 hpi and, for the first time, illustrated a re-distribution of the actin cytoskeleton at 48 hpi (Fig. 3C and 3D). At 48 hpi F-actin presented a polarised localisation at the cell cortex, co-localising with GP64 and mimicking the distribution of GM_1 as detected by CTxB staining at this time (Fig.2C). F-actin and myosin motors have been implicated in the transport of vesicles from the TGN to the plasma membrane (56). Depletion of the F-actin cytoskeleton in AcMNPV-infected cells, via the addition of the actin depolymerising drug LB, resulted in an accumulation of GP64 within the cytoplasm at 24 hpi (Fig. 5), rather than incorporation into the plasma membrane as observed in non-treated samples (Fig. 3C). This supports a similar targeting mechanism for GP64, via F-actin dependent transport vesicle trafficking. The suggestion that GP64, like other virus glycoproteins, may target and accumulate within lipid-raft domains implies a possible role for these structures in the assembly of BV particles at the plasma membrane. The interaction of host F-actin with various raft-associated proteins at the plasma membrane (11, 55, 61, 64) and the possible incorporation of GP64 into raft-domains during infection demonstrated by our results in Figures 1 and 2 suggested the actin cytoskeleton at the cell surface might

also be involved in the budding process of AcMNPV.

Analysis of BV production at 24 hpi in the absence of F-actin revealed decreased titres compared to untreated samples (Fig. 6). We examined whether lowered production of infectious BV was due to reduced trafficking of nucleocapsids to the nucleus following infection or, as proposed by Volkman and others (43, 44, 70), improper packaging of progeny nucleocapsids within the nucleus in the absence of F-actin. RT-PCR confirmed equivalent viral gene transcription in cells treated with LB, confirming that trafficking of nucleocapsids to the nucleus was not demonstrably inhibited in the absence of F-actin. *In vivo* analyses (Table 1) revealed no significant difference in infectivity parameters (lethal dose and survival time) of OBs produced in the presence of LB compared to controls, demonstrating that the production of infectious nucleocapsids and occluded virions within the nucleus were not affected by the depletion of F-actin, in contrast to previous work (43, 44, 70). The presence of plasma membrane-associated GP64 is known to be essential for the production of progeny BV (46) and we propose that the significant decrease of BV production observed in this study in cells treated with LB is due to the deficiency of GP64 in the plasma membrane as a result of an absence of F-actin (Fig. 5). It is logical to suggest that the lack of GP64 at the plasma membrane of F-actin-depleted cells ultimately affected BV production, and that LB interfered with the budding and egress of progeny virus rather than stages involved in the assembly of nucleocapsids in the cell nucleus, as loss of F-actin did not affect the formation of those infectious nucleocapsids embedded in OBs (Table 1). Differences in results compared to earlier work (43, 44, 70) may be due to different mechanisms of the actin destabilising drugs used. The previous studies used cytochalasin D (CD), which may have other, as yet unknown, effects on the baculovirus replication cycle that are not found when using LB.

The results presented here allow an expansion of the current model detailing the trafficking of viral proteins and nucleocapsids within insect cells during baculovirus infection. The accepted model for trafficking of both AcMNPV nucleocapsids and viral proteins should be reviewed and updated and further work is essential to fully understand both the direct and indirect roles of F-actin during late stages of AcMNPV-infection of insect cells.

Acknowledgments

This work was partially supported by a BBSRC grant (LAK, RDP) and by a BBSRC-funded PhD studentship (FJH). We thank Tim Carty for larvae and diet, and Richard Grosvenor for technical assistance.

References

1. **Avisar D, Segal M, Sneh B, *et al.*** 2005. Cell-cycle-dependent resistance to *Bacillus thuringiensis* Cry1C toxin in Sf9 cells. **Cell Sci,** 118: 3463-3171.
2. **Ayres M D, Howard S C, Kuzio J, *et al.*** 1994. The complete DNA sequence of *Autographa californica* nuclear polyhedrosis virus. **Virology,** 202: 586- 605.
3. **Badizadegan K, Wheeler H E, Fujinaga Y, *et al.*** 2004. Trafficking of cholera toxin-ganglioside GM1 complex into Golgi and induction of toxicity depend on actin cytoskeleton. **Am J Physiol Cell Physiol,** 287: 1453-1462.
4. **Berghall H, Wallen C, Hyypia T, *et al.*** 2004. Role of cytoskeleton components in measles virus replication. **Arch. Virol,** 149: 891-901.
5. **Bhattacharya J, Peters P J, Clapham P R.** 2004. Human immunodeficiency virus type 1 envelope glycoproteins that lack cytoplasmic domain cysteines: impact on association with membrane lipid rafts and incorporation into budding virus particles. **J Virol,** 78: 5500-5506.

6. **Blissard G W, Rohrmann G F.** 1989. Location, sequence, transcriptional mapping, and temporal expression of the gp64 envelope glycoprotein gene of *Orgyia pseudotsugata* multicapsid nuclear polyhedrosis virus. **Virology,** 170: 537-555.
7. **Blissard G W, Wenz J R.** 1992. Baculovirus GP64 envelope protein is sufficient to mediate pH-dependent membrane fusion. **J Virol,** 66: 6829- 6835.
8. **Brown D A, London E.** 1998. Functions of lipid rafts in biological membranes. **Ann Rev Cell Develop Biol,** 14: 111-136.
9. **Brown D A, Rose J K.** 1992. Sorting of GPI-anchored proteins to glycolipids-enriched membrane subdomains during transport to the apical cell surface. **Cell,** 68: 533-544.
10. **Brown G, Rixon H W, Sugrue R J.** 2002. Respiratory syncytial virus assembly occurs in GM1-rich regions of the host-cell membrane and alters the cellular distribution of tyrosine phosphorylated caveolin-1. **J Gen Virol,** 83: 1841-1850.
11. **Caroni P.** 2001. Actin cytoskeleton regulation through modulation of PI(4,5)P_2 rafts. **EMBO J,** 20:4332- 4336.
12. **Charlton C A, Volkman L E.** 1986. Effect of tunicamycin on the structural proteins and infectivity of budded *Autographa californica* nuclear polyhedrosis virus. **Virology,** 154: 214-254.
13. **Charlton C A, Volkman L E.** 1991. Sequential arrangement and nuclear polymerisation of actin in baculovirus-infected *Spodoptera frugiperda* cells. **J Virol,** 65: 1219-1227.
14. **Charlton C A, Volkman L E.** 1993. Penetration of *Autographa californica* nuclear polyhedrosis virus nucleocapsids into IPLB Sf 21 cells induces actin cable formation. **Virology,** 197: 245-254.
15. **Chen B J, Takeda M, Lamb R A.** 2005. Influenza virus hemagglutinin (H3 subtype) requires palmitoylation of its cytoplasmic tail for assembly: M1 proteins of two subtypes differ in their ability to support assembly. **J Virol,** 79: 13673-17684.
16. **Chen C, Weisz O A, Stolz D B, *et al.*** 2004. Differential effects of actin cytoskeleton dynamics on equine infectious anaemia virus particle production. **J Virol,** 78: 882-291.
17. **Dreschers S, Roncarati R, Knebel-Morsdorf D.** 2001. Actin rearrangement-inducing factor of baculoviruses is tyrosine phosphorylated and co-localizes to F-actin at the plasma membrane. **J Virol,** 75: 3771-3778.
18. **Eash S, Atwood W J.** 2005. Involvement of cytoskeletal components in BK virus infectious entry. **J. Virol, 79**: 17734-17741.
19. **Goldstein N I, McIntosh A H.** 1980. Glycoproteins of nuclear polyhedrosis viruses. **Arch Virol,** 64: 119-126.
20. **Grzybek M, Kouzek A, Dubielecka P, *et al.*** 2005. Rafts-the current picture. **Folia Histochem Cytobiol,** 43: 3-10.
21. **Haines F J.** 2006. **Trafficking of GP64 and virus egress in AcMNPV-infected insect cells.** PhD Thesis, Oxford Brookes University, Oxford, UK.
22. **Hammarstedt M, Garoff H.** 2004. Passive and active inclusion of host proteins in human immunodeficiency virus type 1 gag particles during budding at the plasma membrane. **J Virol, 78**: 5686-5697.
23. **Han Z, Harty R N.** 2005. Packaging of actin into Ebola virus VLPs. **Virol J,** 2: 92-97.
24. **Henio S, Lusa S, Somerharju P, *et al*.** 2000. Dissecting the role of the Golgi complex and lipid rafts in biosynthetic transport of cholesterol to the cell surface. **Proc Nat Acad Sci USA**, 97: 8375-8380.
25. **Hoehne M, de Couet H G, Stuermer C A, *et al.*** 2005. Loss- and gain-of-function analysis of the lipid raft proteins Reggie/Flotillin in Drosophila: they are posttranslationally regulated, and misexpression interferes with wing and eye development. **Mol Cell Neurosci,** 10: 326-338.
26. **Ikonen E, Simons K.** 1998. Protein and lipid sorting from the trans-Golgi network to the plasma membrane in polarized cells. **Sem Cell Dev Biol,** 9: 503-509.
27. **Jarvis D L A, Garcia A Jr.** 1994. Biosynthesis and Processing of the *Autographa californica* Nuclear Polyhedrosis Virus gp64 Protein. **Virology,** 205: 300-313.
28. **Jarvis D L, Fleming J A, Kovacs G R, *et al.*** 1990. Use of early baculovirus promoters for continuous expression and efficient processing of foreign gene products in stably transformed lepidopteran cells. **Biotech,** 8: 950-955.
29. **Jolly C, Sattentau Q J.** 2005. Human immunodeficiency virus type 1 virological synapse formation in T cells requires lipid raft integrity. **J Virol,** 79: 12088-12094.
30. **Kasman L M, Volkman L E.** 2000. Filamentous actin is required for lepidopteran nucleopolyhedrovirus progeny production. **J. Gen. Virol,** 81: 1881-1888.

31. **Keppler O T, Tibroni N, Venzke S, *et al.*** 2005. Modulation of specific surface receptors and activation sensitization in primary resting $CD4^+$ T lymphocytes by the Nef protein of HIV-1. **J Leukoc Biol,** 79: 616-627.
32. **King L A, Possee R D.** 1992. **Baculovirus Expression System-A Laboratory Guide.** London: Chapman and Hall, UK.
33. **Lambert S, Vind-Kezunovic D, Karvinen S, *et al.*** 2006. Ligand-independent activation of the EGFR by lipid raft disruption. **J Invest Derm,** 126: 954-962.
34. **Lanier L M, Volkman L E.** 1998. Actin binding and nucleation by *Autographa californica* M nucleopolyhedrovirus. **Virology,** 243: 167-177.
35. **LeDuc P R, Whiteley E M, Bao G, *et al.*** 2000. Investigating the secretory pathway of the baculovirus-insect cell system using a secretory green fluorescent protein. **Biotechnol Prog,** 16: 716-723.
36. **Leser G P, Lamb R A.** 2005. Influenza virus assembly and budding in raft-derived microdomains: A quantitative analysis of the surface distribution of HA, NA and M2 proteins. **Virology,** 342: 215-227.
37. **Li M, Yang C, Tong S, *et al.*** 2002. Palmitoylation of the murine leukaemia virus envelope protein is critical for lipid raft association and surface expression. **J Virol,** 76: 11845-11852.
38. **Lindwasser O W, Resh M D.** 2001. Multimerization of human immunodeficiency virus type 1 Gag promotes it localisation to barges, raft-like membrane microdomains. **J Virol,** 75: 7914-7924.
39. **Manié S N, Debreyne S, Vincent S, *et al.*** 2000. Measles virus structural proteins are enriched into lipid raft microdomains: a potential cellular location for virus assembly. **J Virol,** 74: 305-311.
40. **Mazzone A, Tietz P, Jefferson J, *et al.*** 2006. Isolation and characterisation of lipid microdomains from apical and basolateral plasma membrane rat hepatocytes. **Hepatology,** 43: 287-296.
41. **Melkonian K A, Ostermeyer A G, Chen J Z, *et al.*** 1999. Role of lipid modifications in targeting proteins to detergent-resistant membrane rafts. Many raft proteins are acylated, while few are prenylated. **J Biol Chem,** 274: 3910-3917.
42. **Monsma S A, Oomens A G P, Blissard G W, *et al.*** 1996. The GP64 envelope fusion protein is an essential baculovirus protein required for cell-to-cell transmission of infection. **J Virol,** 70: 4607- 4616.
43. **Ohkawa T, Volkman L E.** 1999. Nuclear F-actin is required for AcMNPV nucleocapsid morphogenesis. **Virology,** 264: 1-4.
44. **Ohkawa T, Rowe A R, Volkman L E.** 2002. Identification of six *Autographa californica* multicapsid nucleopolyhedrovirus early genes that mediate nuclear localization of G-actin. **J Virol,** 76: 12281 -12289.
45. **Ono A, Freed E O.** 2001. Plasma membrane rafts play a critical role in HIV-1 assembly and release. **Proc Nat Acad Sci USA,** 98: 13925-13930.
46. **Oomens A G P, Blissard G W.** 1999. Requirement for GP64 to drive efficient budding of *Autographa californica* multicapsid nucleopolyhedrovirus. **Virology,** 254: 297-314.
47. **Oomens A G P, Monsama S A, Blissard G W.** 1995. The Baculovirus GP64 envelope fusion protein: Synthesis, oligomerization and processing. **Virology,** 209: 592-693.
48. **Patmanidi A L, Possee R D, King L A.** 2003. Formation of P10 tubular structures during AcMNPV infection depends of the integrity of host-cell microtubules. **Virology,** 317: 308-320.
49. **Plonksy I, Zimmerberg J.** 1996. The initial fusion pore induced by baculovirus GP64 is large and forms quickly. **J Cell Biol,** 135: 1831-1839.
50. **Plonksy I, Cho M, Oomens A G P, *et al.*** 1999. An analysis of the role of the target membrane on the GP64-induced fusion pore. **Virology,** 253: 65- 76.
51. **Resh M D.** 2004. Membrane targeting of lipid modified signal transduction proteins. **Subcell Biochem,** 37: 217-232.
52. **Roberts T E, Faulkner P.** 1989. Fatty acid acylation of the 67K envelope glycoprotein of a baculovirus: *Autographa californica* nuclear polyhedrosis virus. **Virology,** 172: 377-381.
53. **Roncarati R, Knebel-Mörsdorf D.** 1997. Identification of the early Actin-rearrangement-inducing factor gene, *arif-1*, from *Autographa californica* multicapsid nuclear polyhedrosis virus. **J. Virol,** 71: 7933-7941.
54. **Rousso I, Mixon M B, Chen B K, *et al.*** 2000. Palmitoylation of the HIV-1 envelope glycoprotein is critical for viral infectivity. **Proc Nat Acad Sci USA,** 97: 13523-13525.
55. **Rozelle A L, Machesky L M, Yamamoto M, *et al.*** 2000. Phosphatidylinositol 4,5-bisphosphate induces actin-based

movement of raft-enriched vesicles through WASP-Arp2/3. **Curr Biol,** 10: 331-320.

56. **Satiat-Jeunemaitre B, Cole L, Bourett T, *et al.*** 1996. Brefeldin A effects in plant and fungal cells: something new about vesicle trafficking? **J Microsc,** 181: 162-177.
57. **Scheiffele P, Rietveld A, Wilk T, *et al.*** 1999. Influenza viruses select ordered lipid domains during budding from the plasma membrane. **J Biol Chem,** 274: 2038-2044.
58. **Shenoy-Scaria A M, Dietzen D J, Kwong J, *et al.*** 1994. Cysteine3 of Src family protein tyrosine kinase determines palmitoylation and localization in caveolae. **J Cell Biol,** 126: 353-364.
59. **Simons K, Ikonen E.** 1997. Functional rafts in cell membranes. **Nature,** 387: 569-572.
60. **Simons K, van Meer G.** 1988. Lipid sorting in epithelial cells. **Biochemistry,** 27: 6197-6202.
61. **Simpson-Holley M, Ellis D, Fisher D, *et al.*** 2002. A functional link between the actin cytoskeleton and lipid rafts during budding of filamentous influenza virions. **Virology,** 301: 212-225.
62. **Smith G L, Law M.** 2004. The exit of vaccinia virus from infected cells. **Virus Res,** 106: 189-197.
63. **Spector I, Shocet N R, Kashman Y, *et al.*** 1983. Latrunculins: novel marine toxins that disrupt microfilament organization in cultured cells. **Science,** 219: 493-495.
64. **Stahlhut M, van Deurs B.** 2000. Identification of filamin as a novel ligand for caveolin-1: evidence for the organization of caveolin-1-associated membrane domains by the actin cytoskeleton. **Mol Biol Cell,** 11: 325-337.
65. **Stuermer C A, Plattner H.** 2005. The 'lipid raft' microdomain proteins reggie-1 and reggie-2 (flotillins) are scaffolds for protein interaction and signalling. **Biochem Soc Symp,** 72: 109-118.
66. **Takeda M, Leser G P, Russell C J, *et al.*** 2003. Influenza virus hemagglutinin concentrates in lipid raft microdomains for efficient viral fusion. **Proc Nat Acad Sci USA,** 100: 14610-14617.
67. **Talhouk S N, Volkman L E.**1991. *Autographa californica* M nuclear polyhedrosis virus and cytochalasin D: Antagonists in the regulation of protein synthesis. **Virology,** 182: 626-634.
68. **Thomas C J, Brown H L, Hawes C R, *et al.* 1**998. Localization of a baculovirus-induced chitinase in the insect cell endoplasmic reticulum. **J Virol,** 72: 10207-10212.
69. **Vincent S, Gerlier D, Manié S N.** 2000. Measles virus assembly within membrane rafts. **J Virol,** 74: 9911-9915.
70. **Volkman L E.** 1988. *Autographa californica* MNPV nucleocapsid assembly: inhibition by cytochalasin D. **Virology,** 156: 32-39.
71. **Volkman L E, Goldsmith P A.** 1985. Mechanism of Neutralization of Budded *Autographa californica* Nuclear Polyhedrosis Virus by a Monoclonal Antibody: Inhibition of Entry by Adsorptive Endocytosis. **Virology,** 143: 185- 195.
72. **Volkman L E, Goldsmith P A, Hess R T, *et al.*** 1984. Neutralisation of budded *Autographa californica* NPV by a monoclonal antibody: identification of the target antigen. **Virology,** 133: 354-362.
73. **Whitford M, Stewart S, Kuzio J, *et al.*** 1989. Identification and sequence analysis of a gene encoding gp67, an abundant envelope protein of the *Autographa californica* nuclear polyhedrosis virus. **J Virol,** 63: 1393-1399.
74. **Zhang J, Pekosz A, Lamb R A.** 2000. Influenza virus assembly and lipid raft microdomains; a role for the cytoplasmic tails of the spike glycoproteins. **J Virol,** 74: 4634-4644.
75. **Zhang S, Han Y, Blissard G W.** 2003. Palmitoylation of the *Autographa californica* multicapsid nucleopolyhedrovirus envelope glycoprotein GP64: Mapping, functional studies, and lipid rafts. **J Virol, 77:** 6265-6273.
76. **Zinn K, McAllister L, Goodman C S.** 1988. Sequence analysis and neuronal expression of fasciclin I in grasshopper and *Drosophila*. **Cell,** 53: 577-587.